

# Effective Field Theory Approach to Phase Transitions

Jens O. Andersen

*Department of Physics, The Ohio State University, Columbus, OH 43210*

## Abstract

The effective field theory approach to high temperature field theory can be used to study the phase transition in theories with spontaneously broken symmetry. I construct a sequence of two effective three-dimensional field theories which are valid on successively longer distance scales for a specific model:  $N$  charged  $U(N)$  symmetric scalars coupled to a  $U(1)$  gauge field. The resulting effective Lagrangian can be used to investigate the phase transition, in particular the order of the phase transition as a function of  $N$ , using lattice simulations.

PACS number(s): 11.10.Wx, 12.20.DS, 12.38.Bx

# 1 Introduction

Many problems in quantum field theory at high temperature have been studied extensively since the work of Dolan and Jackiw on symmetry breaking almost twenty five years ago [1]. There has been tremendous progress in perturbative calculations and the methods available for the investigations of quantum systems at high temperature.

Much of the progress has come from separating the effects of different scales. The important scales include the temperature  $T$  and the scale  $gT$  associated with screening lengths and quasi-particle masses. Naive perturbation theory breaks down for soft external momentum  $k$  ( $k \sim gT$ , where  $g$  is some generic coupling constant) because leading order results for some physical quantities (e.g. the gluon damping rate) get contributions from all orders in the loop expansion. This problem can be solved by integrating out the scale  $T$ , which leads to a resummed perturbation theory, which is mainly due to Braaten and Pisarski [2]. Resummation is a reorganization of the ordinary perturbation expansion in which all effects of the scale  $T$  are absorbed into parameters that appear in effective propagators and effective vertices. This reorganization is necessary to do consistent perturbative calculations of real-time processes at high temperature [23].

In the calculation of static quantities such as the free energy (or the effective potential) and screening masses, resummation is just a matter of using an effective propagator. Resummed perturbation theory has been used extensively as a tool for investigating phase transitions at finite temperature. Hebecker has calculated the two-loop effective potential in the abelian Higgs model [3] and Fodor and Hebecker has obtained the effective potential in the standard model, also in the two-loop approximation [4]. In the case of computing static quantities, there exists a simplified resummation scheme due to Arnold and Espinosa, in which only the static modes are dressed by thermal masses [5]. Both the abelian Higgs model and the standard model have been subjects of investigation using this simplified resummation scheme [5]. Resummation has also been used to calculate the free energy in  $g^2\Phi^4$ -theory [6-7], QED [8-10] and QCD [10,11].

Phase transitions, in particular the electroweak phase transition have been investigated by other methods as well. One of these methods is the  $\epsilon$ -expansion. Here, one solves the theory (perturbatively) in  $4 - \epsilon$  dimensions and extrapolate the results to  $\epsilon = 1$  at the end. The  $\epsilon$ -expansion combined with renormalization group methods have been applied in Refs. [12-16].

The strategy of separating scales has proved to be very useful for studying static properties of high temperature field theories. A very powerful method for separating scales is effective field theory [17]. The general idea is to take advantage of one or more well separated mass scales in the problem and treating one scale at a time. This is done by constructing a sequence of effective field theories which are valid on successively longer distance scales and

whose coefficients encode the short-distance physics.

For hot matter, the nonzero Matsubara modes provide the scale  $T$ , while the static modes provide the scale  $gT$  and in some cases (e.g. in nonabelian gauge theories) the scale  $g^2T$  as well [18]. This suggests that one integrates out the nonstatic Matsubara modes to obtain an effective field theory for the zero modes. This effective theory is three-dimensional and the process is the well known dimensional reduction of high temperature field theories [19-21].

The effective field theory approach has been developed into a tool for quantitative calculations by Farakos, Kajantie, Rummukainen and Shaposhnikov [22], and independently by Braaten and Nieto [23]. The idea is that one writes down the most general effective three-dimensional Lagrangian consistent with the symmetries at high temperature. The coefficients in the effective theory is determined by requiring that static correlators in the full theory are reproduced to some desired accuracy by the corresponding correlators in the effective theory at long distances  $R \gg 1/T$ . Moreover, if the effective three-dimensional field theory contains the two momentum scales  $gT$  and  $g^2T$ , one constructs a sequence of two effective field theories by matching correlators at distances  $R \gg 1/(gT)$  [22,23].

The effective field theory approach has been used by Farakos *et al.* [22,24] and by Kajantie *et al.* [25-26] for investigating the important electroweak phase transition which took place in the early Universe. One of the reasons for the interest in the electroweak phase transition is that the baryon asymmetry we observe today, could be a remnant from the phase transition [27,28]. For electroweak matter at temperatures around  $T_c$  there is a hierarchy of three momentum scales, and so the first step is to construct a sequence of two effective field theories [22]. The second step is the application of the three-dimensional effective field theory. Normally, the perturbation expansion breaks down at temperatures close to  $T_c$ , so one must use nonperturbative methods such as lattice simulations. This has been carried out in [24-26]. The conclusion of their investigation is that the electroweak phase transition in the standard model is not sufficiently strongly first order for realistic values of the Higgs mass to produce the present baryon asymmetry, and one must consider extensions such as the minimal supersymmetric standard model [22,24-26,29].

Effective field theory methods have been used by Braaten and Nieto [30] to solve the long-standing infrared catastrophe of QCD [31]. It is a well-known fact that the free energy of nonabelian gauge theories cannot be calculated beyond fifth order in the coupling using resummed perturbation theory. The method breaks down at order  $g^6$ , due to infrared divergences, as first pointed out by Linde [31]. These divergences arise from regions where all internal energies vanish, and so the singularities are the same as in three-dimensional pure QCD. Thus, the breakdown of perturbation theory simply reflects the infrared problems appearing in a perturbative treatment of any nonabelian gauge theory in three dimensions. Using the effective field theory approach one can compute order by order in the gauge cou-

pling  $g$  the contributions to the free energy, although some coefficients must be evaluated numerically. The infrared problems can naturally be avoided if one uses lattice simulations directly in four dimensions. However, this is extremely time consuming in comparison with three-dimensional calculations and the time savings here arise from the reduction of the problem from four to three dimensions, and also by integrating out the fermions.

Effective field theory has also been used to organize perturbative calculations of the free energy in  $g^2\Phi^4$ -theory [23], QED [32] and SQED [33]. Moreover, it has also been used for carrying out perturbative calculations of screening lengths in the same theories [23,32,33].

In the present work we apply effective field theory methods to construct an effective three-dimensional field theory which can be used in the study of phase transitions for a specific field theory: a  $U(1)$  gauge theory coupled to  $N$  charged  $U(N)$  symmetric scalars. This is simply scalar electrodynamics where the scalar field is an  $N$ -component complex vector, and we shall refer to this model as SQED in the following. For  $N = 1$ , the effective field theory has already been constructed by Farakos *et al.* in Ref. [22], and several aspects of the phase transition have been studied numerically by Karjalainen, Laine and Peisa [34], and by Kajantie, Karjalainen, Laine and Peisa [35]. Moreover, this theory has previously been investigated by Arnold [12] and Lawrie [13] using the  $\epsilon$ -expansion. This method indicates that the order of the phase transition depends on the number of scalar fields  $N$ . Numerical study of the effective field theory obtained in the present paper, would give valuable information on the applicability of the  $\epsilon$ -expansion.

The plan of the article is as follows. In section II we review the ideas behind dimensional reduction and the construction of effective three-dimensional field theories. In section III and IV we determine the coefficients in the two effective field theories arising in our model. In section V we summarize and conclude. In Appendix A and B, the notation and conventions are given. We also list the sum-integrals in the full theory as well as the integrals in the effective theories which are needed in the present work.

## 2 Dimensional Reduction and Effective Field Theories

In this section we briefly discuss the ideas behind dimensional reduction and the effective field theory approach to phase transitions at finite temperature.

The specific model we study in the present work is a  $U(N)$  symmetric complex scalar field coupled to an abelian gauge field. The Euclidean Lagrangian for SQED reads

$$\mathcal{L}_{\text{SQED}} = \frac{1}{4}F_{\mu\nu}F_{\mu\nu} + (\mathcal{D}_\mu\Phi)^\dagger(\mathcal{D}_\mu\Phi) + \nu^2\Phi^\dagger\Phi + \frac{\lambda}{6}(\Phi^\dagger\Phi)^2 + \mathcal{L}_{\text{gf}} + \mathcal{L}_{\text{gh}}. \quad (1)$$

Here  $D_\mu = \partial_\mu + ieA_\mu$  is the covariant derivative and  $\Phi^\dagger = (\Phi_1^\dagger, \Phi_2^\dagger, \dots, \Phi_N^\dagger)$ .  $\Phi$  is the corre-

sponding column vector. In the present work, we perform the calculations in the Landau gauge. This is merely a convenient choice, since many of the diagrams vanish in this gauge. Our final results are of course gauge-invariant.

In the imaginary time formalism bosonic fields are periodic in the time direction with period  $\beta$ , while fermionic fields are antiperiodic with the same period. This allows one to decompose the fields into their Fourier components, which are characterized by their Matsubara frequencies. For bosonic fields these are  $2n\pi T$  and for fermions they are  $(2n + 1)\pi T$ . The Matsubara frequencies act as masses for the Fourier components of the fields, and one can view a four-dimensional field theory at finite temperature as a three-dimensional field theory at zero temperature with an infinite tower of fields [19]. Thus, the nonzero Matsubara modes have masses of order  $T$ , while the static mode of  $A_0$  acquires a thermal mass of order  $gT$ . The zero mode of  $A_i$  is massless (there is no magnetic mass in abelian gauge theories) and if the temperature is close to the critical temperature the static modes of the scalar fields have masses of order  $g^2T$ . Hence, there is a hierarchy of three momentum scales,  $T$ ,  $gT$  and  $g^2T$  which are well separated in the weak coupling limit. This suggests that one construct a sequence of two effective field theories which are valid on successively longer distance scales: The first step is to integrate out the nonzero Matsubara frequencies and construct an effective three-dimensional field theory for the  $n = 0$  bosonic modes. This is the familiar process of dimensional reduction of hot field theories [19-21]. The second effective field theory is obtained by integrating out the timelike component of the gauge field [22,23].

The first effective field theory is called electrostatic scalar electrodynamics (ESQED) and the fields can be approximately identified with the zero-frequency modes of the original fields.  $\mathcal{L}_{\text{ESQED}}$  consists of a real massive scalar field, which can be identified with the zero mode of the temporal component of the gauge field. We denote this field by  $\rho$ . Moreover, we have the  $N$ -component scalar field  $\phi$  and the three-dimensional gauge field  $A_i^{3d}$  which are associated with the zero-frequency modes of  $\Phi$  and  $A_i$  in SQED, respectively. We can then schematically write

$$\phi(\mathbf{x}) \approx \sqrt{T} \int_0^\beta d\tau \Phi(\mathbf{x}, \tau), \quad A_i^{3d}(\mathbf{x}) \approx \sqrt{T} \int_0^\beta d\tau A_i(\mathbf{x}, \tau), \quad \rho(\mathbf{x}) \approx \sqrt{T} \int_0^\beta d\tau A_0(\mathbf{x}, \tau). \quad (2)$$

The symmetries are as follows: There is a gauged  $U(N)$  symmetry of  $\phi$  and a  $Z_2$ -symmetry of  $\rho$ . Hence, the Lagrangian of ESQED is

$$\begin{aligned} \mathcal{L}_{\text{ESQED}} = & \frac{1}{4} F_{ij} F_{ij} + (\mathcal{D}_i \phi)^\dagger (\mathcal{D}_i \phi) + M^2(\Lambda) \phi^\dagger \phi + \frac{\lambda_E(\Lambda)}{6} (\phi^\dagger \phi)^2 + \frac{1}{2} (\partial_i \rho)^2 \\ & + \frac{1}{2} m_E^2(\Lambda) \rho^2 + \frac{\lambda_A(\Lambda)}{24} \rho^4 + h_E^2(\Lambda) \phi^\dagger \phi \rho^2 + \mathcal{L}_{\text{gf}} + \mathcal{L}_{\text{gh}} + \delta \mathcal{L}. \end{aligned} \quad (3)$$

The parameters in ESQED are called *short-distance coefficients*. The term  $\delta \mathcal{L}_{\text{ESQED}}$  represents all other terms in ESQED which can be constructed out of the fields and which respect the symmetries. Examples of such terms are  $h(\Lambda) \rho^2 F_{ij}^2$  and  $g(\Lambda) (\phi^\dagger \phi)^3 \rho^2$ .

The second three-dimensional effective field theory is named magnetostatic scalar electrodynamics (MSQED) and consists of the fields  $\tilde{\phi}$  and  $\tilde{A}_i^{3d}$ . The fields in MSQED are to a first approximation identified with the fields in ESQED. The symmetry is a gauged  $U(N)$  symmetry, exactly as in full SQED. The Lagrangian of MSQED then reads

$$\mathcal{L}_{\text{MSQED}} = \frac{1}{4}F_{ij}F_{ij} + (\mathcal{D}_i\tilde{\phi})^\dagger(\mathcal{D}_i\tilde{\phi}) + \tilde{M}^2(\Lambda)\tilde{\phi}^\dagger\tilde{\phi} + \frac{\lambda_M(\Lambda)}{6}(\tilde{\phi}^\dagger\tilde{\phi})^2 + \mathcal{L}_{\text{gf}} + \mathcal{L}_{\text{gh}} + \delta\mathcal{L}_{\text{MSQED}}. \quad (4)$$

The parameters of MSQED are termed *middle-distance coefficients*. The term  $\delta\mathcal{L}_{\text{MSQED}}$  includes all operators that can be made out of  $\tilde{A}_i$  and  $\tilde{\phi}$ , for instance  $c(\Lambda)(F_{ij}F_{ij})^2$ .

In the equations above, we have indicated that the parameters generally depend on  $\Lambda$ , which is the ultraviolet cutoff of the effective theory. This cutoff dependence is necessary in order to cancel the  $\Lambda$ -dependence which arises in perturbative calculations using the effective theory.

Matching static Greens functions in SQED and ESQED is complicated by the breakdown of the relation (2) between the fields in the fundamental theory and the fields in the effective theory. In the present case this breakdown takes place at leading order in  $e^2$  and we must allow for short-distance coefficients multiplying the fields  $\phi$ ,  $A_i^{3d}$  and  $\rho$  in ESQED [23]. These short-distance coefficients are associated with field strength renormalization of the fundamental fields. They can be found by computing the momentum dependent part of the propagator of the relevant fields [22,24]. In the one-loop approximation, we denote these coefficients by  $\Sigma^{(1)'}(0)$ ,  $\Pi^{(1)'}(0)$  and  $\Pi_{00}^{(1)'}(0)$  (see subsection 3.1). The relations between the fields in SQED and ESQED at leading order in  $\lambda$  and  $e^2$

$$\left[1 - \Sigma^{(1)'}(0)\right]\phi(\mathbf{x}) \approx \sqrt{T} \int_0^\beta d\tau \Phi(\mathbf{x}, \tau), \quad (5)$$

$$\left[1 - \Pi^{(1)'}(0)\right]A_i^{3d}(\mathbf{x}) \approx \sqrt{T} \int_0^\beta d\tau A_i(\mathbf{x}, \tau), \quad (6)$$

$$\left[1 - \Pi_{00}^{(1)'}(0)\right]\rho(\mathbf{x}) \approx \sqrt{T} \int_0^\beta d\tau A_0(\mathbf{x}, \tau). \quad (7)$$

The above remarks also apply when we match correlators in ESQED and MSQED, although the middle-distance coefficients vanish at one-loop (see subsection 4.1).

Let us close this section by motivating the study of this field theory given by (1). In the introduction we mentioned that the order of the phase transition may depend on the number of scalars  $N$  in the theory. These expectations arise from the study of the  $\epsilon$ -expansion [12]. The  $\epsilon$ -expansion generalizes the three spatial dimensions to  $4 - \epsilon$  dimensions. One solves the theory when  $\epsilon$  is small and then extrapolates to three dimensions, i.e. to  $\epsilon = 1$ . The  $\epsilon$ -expansion is not necessarily well behaved at  $\epsilon = 1$ . For pure  $g^2\Phi^4$ , it is very successful and has predicted critical exponents in good agreement with other methods [12].

The infrared behaviour can be studied by looking at the renormalization group flow of the couplings of the relevant operators. The one-loop renormalization group equations in  $4 - \epsilon$  dimensions read [12]:

$$\Lambda \frac{de^2}{d\Lambda} = \epsilon e^2 - \frac{Ne^4}{24\pi^2}, \quad (8)$$

$$\Lambda \frac{d\lambda}{d\Lambda} = \epsilon \lambda - \frac{(N+4)\lambda - 18\lambda e^2 + 54e^4}{24\pi^2}, \quad (9)$$

The point is that the renormalization group equations have a nontrivial infrared fixed point in  $4 - \epsilon$  dimensions for  $N > N_c$ , where  $N_c \approx 365.9$ . Such fixed points are taken as evidence for a second order phase transition, since the theory looks the same on all distance scales [5]. According to Ref. [12], the  $\epsilon$ -expansion is not so well behaved when the number of fields  $N$  become large. So it is of great interest to study this system by other means. The results presented in this work provide a first step in this direction.

### 3 Short-distance Coefficients

In this section we determine the short-distance coefficients  $m_E^2(\Lambda)$  and  $M^2(\Lambda)$  to next-to-leading order in the parameters  $\nu^2$ ,  $\lambda$  and  $e^2$ . We also compute the parameters  $\lambda_E(\Lambda)$ ,  $e_E^2(\Lambda)$  and  $h_E^2(\Lambda)$  to next-to-leading order, as well as the coefficient  $\lambda_A(\Lambda)$  to leading order.

In the present work we shall use naive or *strict perturbation* [23] to determining the parameters in the effective theory. The Lagrangian of SQED is split according to

$$\begin{aligned} (\mathcal{L}_{\text{SQED}})_0 &= \frac{1}{4}F_{\mu\nu}F_{\mu\nu} + (\partial_\mu\Phi)^\dagger(\partial_\mu\Phi) + \mathcal{L}_{\text{gf}} + \mathcal{L}_{\text{gh}}, \\ (\mathcal{L}_{\text{SQED}})_{\text{int}} &= \nu^2\Phi^\dagger\Phi + e^2\Phi^\dagger\Phi A_\mu^2 - ieA_\mu(\Phi^\dagger\partial_\mu\Phi - \Phi\partial_\mu\Phi^\dagger) + \frac{\lambda}{6}(\Phi^\dagger\Phi)^2. \end{aligned} \quad (10)$$

Although the strict perturbation expansion breaks down at distance scales  $R \gg 1/T$ , we can use it as device determining the short-distance coefficients in the effective Lagrangian. The idea is that physical quantities receive contributions from three momentum scales  $T$ ,  $eT$  and  $e^2T$ . The parameters of ESQED are insensitive to the scales  $eT$  and  $e^2T$  but encode the physics at the scale  $T$ . However, in the matching calculations we must make the same incorrect assumptions about the long-distance behaviour in the effective theory. If we tune the parameters so that the two theories are equal at long distances, then the infrared divergences in full SQED are identical to those encountered in ESQED. Of course, in perturbative calculations, one must regularize the infrared divergences by an infrared cutoff. In the present work dimensional regularization is used. In the effective theory these incorrect assumptions amount to treating the mass parameters as well as other operators as perturbations. Strict

perturbation theory is then defined by the following decomposition of the Lagrangian of ESQED

$$\begin{aligned}
(\mathcal{L}_{\text{ESQED}})_0 &= \frac{1}{4}F_{ij}F_{ij} + (\partial_i\phi^\dagger)(\partial_i\phi) + \frac{1}{2}(\partial_i\rho)^2 + \mathcal{L}_{\text{gf}} + \mathcal{L}_{\text{gh}}, \\
(\mathcal{L}_{\text{ESQED}})_{\text{int}} &= M^2(\Lambda)\phi^\dagger\phi + \frac{1}{2}m_E^2(\Lambda)\rho^2 + \frac{\lambda_E(\Lambda)}{6}(\phi^\dagger\phi)^2 + e_E^2(\Lambda)\phi^\dagger\phi A_i^2 + \\
&\quad h_E^2(\Lambda)\phi^\dagger\phi\rho^2 + ie_E(\Lambda)A_i(\phi^\dagger\partial_i\phi - \phi\partial_i\phi^\dagger) + \frac{\lambda_A(\Lambda)}{24}\rho^4 + \delta\mathcal{L}. \quad (11)
\end{aligned}$$

In full SQED, wiggly and solid lines denote the propagators of photons and charged scalars, respectively. In ESQED, the same conventions apply. Moreover, dashed lines denote the propagators of the real scalar field  $\rho$ . A cross in the Feynman diagrams denotes the insertion of the operator  $\nu^2$ . Note also that the figures only display those diagrams in the perturbative expansion which are non-vanishing in the Landau gauge.

### 3.1 Field Normalization Constants

In this subsection we compute the short-distance coefficients  $\Sigma^{(1)'}(0)$ ,  $\Pi^{(1)'}(0)$  and  $\Pi_{00}^{(1)'}(0)$  which multiply the fields  $\phi$ ,  $A_i^{3d}$  and  $\rho$  in ESQED.

We denote the *static* self-energy function of the scalar field by  $\Sigma(\mathbf{k})$ , and the static polarization tensor of the gauge field by  $\Pi_{\mu\nu}(\mathbf{k})$ . Now,  $\Sigma(\mathbf{k})$  and  $\Pi_{\mu\nu}(\mathbf{k})$  can be expanded in number of loops in the loop expansion and can also be expanded in powers of the external momentum  $\mathbf{k}$ . If we denote the  $n$ 'th order contribution to the scalar self-energy function by  $\Sigma^{(n)}(\mathbf{k})$ , we can write

$$\Sigma(\mathbf{k}) = \Sigma^{(1)}(0) + k^2\Sigma^{(1)'}(0) + \Sigma^{(2)}(0) + \mathcal{O}(k^4/T^2). \quad (12)$$

The corresponding relations for the various component of the photon polarization tensor read

$$\Pi_{00}(\mathbf{k}) = \Pi_{00}^{(1)}(0) + k^2\Pi_{00}^{(1)'}(0) + \Pi_{00}^{(2)}(0) + \mathcal{O}(k^4/T^2), \quad (13)$$

$$\Pi_{ij}(\mathbf{k}) = (k^2\delta_{ij} - k_ik_j)\Pi^{(1)'}(0) + \mathcal{O}(k^4/T^2). \quad (14)$$

The fact that the infrared limit of  $\Pi_{ij}(\mathbf{k})$  is zero reflects that spatial magnetic fields are not screened in the plasma.

The one-loop diagrams contributing to the self-energy of the scalar field are shown in Fig. 11, and read

$$\begin{aligned}
\Sigma^{(1)}(\mathbf{k}) &= \frac{\nu^2(N+1)\lambda}{3}\int_{\mathcal{P}} \frac{1}{P^4} + \frac{(N+1)\lambda}{3}\int_{\mathcal{P}} \frac{1}{P^2} + (d-1)e^2\int_{\mathcal{P}} \frac{1}{P^2} \\
&\quad - e^2\int_{\mathcal{P}} \frac{4k^2}{P^2(P+K)^2} - e^2\int_{\mathcal{P}} -\frac{4(\mathbf{p}\mathbf{k})^2}{P^4(P+K)^2}. \quad (15)
\end{aligned}$$

Expanding in powers of the external momentum  $\mathbf{k}$  gives

$$\begin{aligned}\Sigma^{(1)}(\mathbf{k}) &= \frac{\nu^2(N+1)\lambda}{3} \not\int_P \frac{1}{P^4} + \frac{(N+1)\lambda}{3} \not\int_P \frac{1}{P^2} + e^2(d-1) \not\int_P \frac{1}{P^2} \\ &\quad - 3e^2k^2 \not\int_P \frac{1}{P^4} + \mathcal{O}(k^4/T^2).\end{aligned}\tag{16}$$

From (16) we immediately get

$$\Sigma^{(1)}(0) = \frac{\nu^2(N+1)\lambda}{3} \not\int_P \frac{1}{P^4} + \frac{(N+1)\lambda}{3} \not\int_P \frac{1}{P^2} + e^2(d-1) \not\int_P \frac{1}{P^2},\tag{17}$$

$$\Sigma^{(1)'}(0) = -3e^2 \not\int_P \frac{1}{P^4} + \mathcal{O}(k^4/T^2).\tag{18}$$

The sum-integral in (18) is ultraviolet divergent and the divergence is removed by the field strength renormalization counterterm, To leading order we have

$$Z_\Phi = 1 + \frac{3e^2}{16\pi^2\epsilon}.\tag{19}$$

We then obtain

$$\Sigma^{(1)'}(0) = \frac{3e^2}{(4\pi)^2} (\ln \frac{\Lambda}{4\pi T} + \gamma_E).\tag{20}$$

Let us next move to the gauge field. The one-loop diagrams which contribute to the photon polarization tensor are displayed in Fig. 12. The calculations are straightforward, and one finds

$$\Pi_{00}^{(1)}(0) = 2Ne^2 \not\int_P \frac{1}{P^2} - 4Ne^2 \not\int_P \frac{p_0^2}{P^4},\tag{21}$$

$$\Pi_{00}^{(1)'}(0) = \frac{4Ne^2}{3} \not\int_P \frac{p_0^2}{P^6},\tag{22}$$

$$\Pi^{(1)'}(0) = \frac{Ne^2}{3} \not\int_P \frac{1}{P^4}.\tag{23}$$

Similarly, we carry out wave function renormalization of the gauge field by employing

$$Z_A = 1 - \frac{Ne^2}{48\pi^2\epsilon}.\tag{24}$$

This yields

$$\Pi_{00}^{(1)'}(0) = \frac{Ne^2}{3(4\pi)^2} (\ln \frac{\Lambda}{4\pi T} + \gamma_E + 1),\tag{25}$$

$$\Pi^{(1)'}(0) = \frac{Ne^2}{3(4\pi)^2} (\ln \frac{\Lambda}{4\pi T} + \gamma_E).\tag{26}$$

### 3.2 Coupling Constants

In this subsection we shall determine the coupling constants  $\lambda_E(\Lambda)$ ,  $e_E^2(\Lambda)$  and  $h_E^2(\Lambda)$  to next-to-leading order in the coupling constants of the full theory. We also compute the coupling constant  $\lambda_A(\Lambda)$  to leading order. For  $N = 1$  these parameters have been calculated in [22].

Let us first consider the coefficient  $\lambda_E(\Lambda)$ . To leading order one can simply read off this parameter from the full theory. Substituting  $\Phi(\mathbf{x}, \tau) \rightarrow \sqrt{T}\phi(\mathbf{x})$  into (1) and comparing  $\int_0^\beta d\tau \mathcal{L}_{\text{SQED}}$  with the Lagrangian of ESQED we find

$$\lambda_E(\Lambda) = \lambda T. \quad (27)$$

One way to calculate the coupling  $\lambda_E(\Lambda)$  beyond leading order, is by matching the static four-point function of the Higgs field in full SQED with the four-point function of the Higgs field in ESQED. This is complicated by the breakdown of the simple relation (20) At next-to-leading order it is sufficient to take into account the short-distance coefficient which multiplies  $\phi$ .

We denote the four-point of the Higgs field in SQED by  $\Gamma_{\phi_1, \phi_1, \phi_1, \phi_1}^{\text{SQED}}(\mathbf{k})$ , where  $\mathbf{k}$  collectively denotes the external momenta. The one-loop correction to the four-point function is given by the Feynman diagrams in Fig. 13. Taken at zero external momenta, one finds

$$\Gamma_{\phi_1, \phi_1, \phi_1, \phi_1}^{\text{SQED}}(0) = \lambda - \frac{(N+4)}{3} \lambda^2 \int_K \frac{1}{K^4} - 6(d-1)e^4 \int_K \frac{1}{K^4}. \quad (28)$$

In ESQED, we denote the corresponding four-point function by  $\Gamma_{\phi_1, \phi_1, \phi_1, \phi_1}^{\text{ESQED}}(\mathbf{k})$ . Since all the fields are massless in the strict perturbation expansion and all diagrams are taken at vanishing external momenta, there is no scale in the integrals. Thus the loop corrections to  $\Gamma_{\phi_1, \phi_1, \phi_1, \phi_1}^{\text{ESQED}}(0)$  vanish:

$$\Gamma_{\phi_1, \phi_1, \phi_1, \phi_1}^{\text{ESQED}}(0) = \lambda_E(\Lambda). \quad (29)$$

Taking into account the short-distance coefficient multiplying the field  $\phi$  (note that we use the unrenormalized coefficient), the matching leads to the following equation

$$\lambda_E(\Lambda) = \lambda T - \frac{(N+4)}{3} \lambda^2 T \int_K \frac{1}{P^4} + 6\lambda e^2 T \int_P \frac{1}{P^4} - 6(d-1)e^4 T \int_P \frac{1}{P^4}. \quad (30)$$

Renormalization of the quartic coupling  $\lambda$  is carried out by the substitution  $\lambda \rightarrow Z_\lambda \lambda$  in the first term on the right hand side of (30), where

$$Z_\lambda = 1 + \frac{(N+4)\lambda - 18\lambda e^2 + 54e^4}{3(4\pi)^2 \epsilon}. \quad (31)$$

This yields

$$\lambda_E(\Lambda) = T \left[ \lambda - \frac{(N+4)\lambda^2 - 18\lambda e^2 + 54e^4}{24\pi^2} \left( \ln \frac{\Lambda}{4\pi T} + \gamma_E \right) + \frac{3e^4}{4\pi^2} \right]. \quad (32)$$

The couplings  $e_E^2(\Lambda)$  and  $h_E^2(\Lambda)$  are computed by matching the correlators  $\Gamma_{\Phi_1^\dagger\Phi_1 A_i A_j}^{\text{SQED}}(\mathbf{k})$  and  $\Gamma_{\Phi_1^\dagger\Phi_1 A_0 A_0}^{\text{SQED}}(\mathbf{k})$  in full SQED with the corresponding correlators in ESQED. The relevant diagrams are displayed in Fig. 14. Calculated at zero external momenta one finds the following results in SQED in the one-loop approximation:

$$\Gamma_{\Phi_1^\dagger\Phi_1 A_i A_j}^{\text{SQED}}(0) = e^2 + 8e^4 \not\int_P \left[ \frac{p_i p_j}{P^6} - \frac{1}{P^4} \right] + \frac{\lambda e^2 (N+3)}{3} \not\int_P \left[ 4 \frac{p_i p_j}{P^6} - \frac{1}{P^4} \right], \quad (33)$$

$$\Gamma_{\Phi_1^\dagger\Phi_1 A_0 A_0}^{\text{SQED}}(0) = e^2 + 8e^4 \not\int_P \left[ \frac{p_0^2}{P^6} - \frac{1}{P^4} \right] + \frac{\lambda e^2 (N+3)}{3} \not\int_P \left[ 4 \frac{p_0^2}{P^6} - \frac{1}{P^4} \right]. \quad (34)$$

In MSQED we know that the one-loop correction to the correlators vanish, since all internal fields are massless and the external momenta are zero. Taking into account the short-distance coefficients multiplying the  $3d$  fields and carrying out charge renormalization, using

$$Z_{e^2} = 1 + \frac{N e^2}{3(4\pi)^2 \epsilon}, \quad (35)$$

we end up with

$$e_E^2(\Lambda) = e^2 T \left[ 1 - \frac{N e^2}{24\pi^2} \left( \ln \frac{\Lambda}{4\pi T} + \gamma_E \right) \right], \quad (36)$$

$$h_E^2(\Lambda) = e^2 T \left[ 1 - \frac{N e^2}{24\pi^2} \left( \ln \frac{\Lambda}{4\pi T} + \gamma_E + 1 \right) + \frac{\lambda(N+3)}{48\pi^2} + \frac{e^2}{8\pi^2} \right]. \quad (37)$$

We close this subsection by computing the coefficient in front of the operator  $\rho^4$ . To leading order in the couplings of full SQED,  $\lambda_A(\Lambda)$  is given by the one-loop contribution to the four-point function for timelike photons at zero external momenta. This correlator is denoted by  $\Gamma_{A_0 A_0 A_0 A_0}^{\text{SQED}}(\mathbf{k})$ . The matching condition then reads

$$\lambda_A(\Lambda) = T \Gamma_{A_0 A_0 A_0 A_0}^{\text{SQED}}(0). \quad (38)$$

The one-loop graphs contributing to this correlator are displayed in Fig. 15. One obtains

$$\Gamma_{A_0 A_0 A_0 A_0}^{\text{SQED}}(\mathbf{k}) = -12 N e^4 \not\int_P \frac{1}{P^4} + 96 N e^4 \not\int_P \frac{p_0^2}{P^6} - 96 N e^4 \not\int_P \frac{p_0^4}{P^8}. \quad (39)$$

Again the sum-integrals are divergent term by term, but the poles in  $\epsilon$  cancel in the final result. This is also the case in QED and QCD [19]. Using Appendix A, we find

$$\lambda_A(\Lambda) = \frac{N e^4 T}{\pi^2}. \quad (40)$$

Finally, we note that the four coupling constants  $\lambda_E(\Lambda)$ ,  $e_E^2(\Lambda)$ ,  $h_E^2(\Lambda)$  and  $\lambda_A(\Lambda)$  are renormalization group invariant at next-to-leading order in the coupling constants of SQED. Thus, we can trade the scale  $\Lambda$  for arbitrary renormalization scale  $\mu$ .

### 3.3 Mass parameters

In this subsection we calculate the mass parameters  $M^2(\Lambda)$  and  $m^2(\Lambda)$  in the effective Lagrangian at next-to-leading order in  $\nu^2$ ,  $\lambda$  and  $e^2$ . The leading order results for  $N = 1$  can be found in e.g. [22], while the result for  $m^2(\Lambda)$  at next-to-leading order has been obtained in [33]. There are several ways of determining the mass parameters. One way is to match the propagator of the zero-frequency mode in the full theory with the propagator in ESQED.

Let us denote the static two-point function of the Higgs field in SQED by  $\Gamma_{\phi_1\phi_1}^{\text{SQED}}(\mathbf{k})$ . Since we can expand the self-energy function in both powers of the external momentum and number of loops we can write

$$\Gamma_{\phi_1\phi_1}^{\text{SQED}}(\mathbf{k}) = k^2 + \nu^2 + \Sigma^{(1)}(\mathbf{k}) + k^2\Sigma^{(1)'}(\mathbf{k}) + \Sigma^{(2)}(\mathbf{k}). \quad (41)$$

Similarly, we denote the two-point function of the Higgs field in ESQED by  $\Gamma_{\phi_1\phi_1}^{\text{ESQED}}(\mathbf{k})$ . We can then write

$$\Gamma_{\phi_1\phi_1}^{\text{ESQED}}(\mathbf{k}, \Lambda) = k^2 + M^2(\Lambda) + \delta M^2. \quad (42)$$

Here, we have added a mass counterterm  $\delta M^2$ , which is associated with mass renormalization. The matching requirement is then

$$\Gamma_{\phi_1\phi_1}^{\text{SQED}}(\mathbf{k}) = [1 + \Sigma^{(1)'}(0)]\Gamma_{\phi_1\phi_1}^{\text{ESQED}}(\mathbf{k}) \quad (43)$$

The factor  $[1 + \Sigma^{(1)'}(0)]$  is a consequence of the short-distance coefficient that multiplies the field  $\phi$ . Solving for the mass parameter, we obtain

$$M^2(\Lambda) = -\nu^2[1 - \Sigma^{(1)'}(0)] + \Sigma^{(1)}(0)[1 - \Sigma^{(1)'}(0)] + \Sigma^{(2)}(0) - \delta M^2. \quad (44)$$

$\Sigma^{(1)}(0)$  and  $\Sigma^{(1)'}(0)$  are given by (17) and (18). The two-loop contributions to the scalar self-energy are depicted in Fig. 16 and yield

$$\begin{aligned} \Sigma^{(2)}(0) = & -\frac{(N+1)^2\lambda^2}{9} \not\int_{PQ} \frac{1}{P^2Q^4} - 2(d-2)Ne^4 \not\int_{PQ} \frac{1}{P^2Q^4} - \\ & (d-1)\frac{(N+1)\lambda e^2}{3} \not\int_{PQ} \frac{1}{P^2Q^4}. \end{aligned} \quad (45)$$

The parameter  $\nu^2$  is renormalized by the substitution [5]

$$Z_{\nu^2} = 1 + \frac{(N+1)\lambda}{3(4\pi)^2\epsilon} - \frac{3e^2}{(4\pi)^2\epsilon}, \quad (46)$$

while the renormalization constants for  $\lambda$  and  $e^2$  are given by (31) and (35). We are still left with a pole in  $\epsilon$ . This divergence is cancelled by the mass counterterm, which thereby is determined to be

$$\delta M^2 = \frac{(N+1)\lambda^2 T^2 - 6(N+1)\lambda e^2 T^2 + 9(N+5)e^4 T^2}{36(4\pi)^2\epsilon}. \quad (47)$$

It is also convenient to express the mass parameter in terms of the coupling constants of ESQED that we obtained in the previous subsection. This gives the mass parameter  $M^2(\Lambda)$  to two-loop order:

$$M^2(\Lambda) = \tilde{\nu}^2(\mu) + \frac{(N+1)\lambda_E(\mu)T^2}{36} + \frac{e_E^2(\mu)T^2}{4} + \frac{(N+1)\lambda e^2 T^2}{18(4\pi)^2} - \frac{(N+15)e^4 T^2}{18(4\pi)^2} - \left( \frac{(N+1)\lambda^2 T^2 - 6(N+1)\lambda e^2 T^2 + 9(N+5)e^4}{9(4\pi)^2} \right) \left( \ln \frac{3T}{\Lambda} + c \right). \quad (48)$$

Here, the renormalization group invariant mass parameter  $\tilde{\nu}^2(\mu)$  is

$$\tilde{\nu}^2(\mu) = \nu^2 \left\{ 1 + \frac{1}{(4\pi)^2} \left[ 6e^2 - \frac{2(N+1)\lambda}{3} \right] \left( \ln \frac{\mu}{4\pi T} + \gamma_E \right) \right\} \quad (49)$$

and the constant  $c$  introduced in [25] is

$$\begin{aligned} c &= \frac{1}{2} \ln \frac{8\pi}{9} + \frac{1}{2} \frac{\zeta'(2)}{\zeta(2)} - \gamma_E \\ &= \ln \frac{3}{4\pi} + \frac{1}{2} + \frac{1}{2} \frac{\zeta'(-1)}{\zeta(-1)} \\ &\approx -0.348725. \end{aligned}$$

Note that we have used the renormalization group equations [5],

$$\mu \frac{d\lambda}{d\mu} = \frac{(N+4)\lambda^2 - 18\lambda e^2 + 54e^4}{24\pi^2}, \quad \mu \frac{de^2}{d\mu} = \frac{Ne^4}{24\pi^2}, \quad (50)$$

to change the scale from  $\Lambda$  to  $\mu$ . There is a remaining dependence on  $\Lambda$ , which shows that  $M^2(\Lambda)$  depends explicitly upon the factorization scale  $\Lambda$ . This is necessary in order to cancel the  $\Lambda$ -dependence which arises in the effective theory.

Let us now turn to the mass parameter  $m_E^2(\Lambda)$ . This parameter is determined by matching the propagator of the zero-frequency mode of the timelike component of the gauge with the propagator of the real scalar field  $\rho$  in ESQED. In complete analogy with the calculations of the scalar mass parameter, we find

$$m_E^2(\Lambda) = \Pi_{00}^{(1)}(0) + \Pi_{00}^{(2)}(0) - \Pi_{00}^{(1)'}(0)\Pi_{00}^{(1)}(0). \quad (51)$$

Now, the expressions for  $\Pi_{00}^{(1)}(0)$  and  $\Pi_{00}^{(1)'}(0)$  are given by (21) and (22), while the two-loop part of the self-energy of  $A_0$  is given by the displayed graphs in Fig. 17. Many of the two-loop sum-integrals vanish in dimensional regularization, while others factorize into products of one-loop sum-integrals. After some calculations we find

$$\begin{aligned} \Pi_{00}^{(2)}(0) &= 8(d-1)Ne^4 \not\int_{PQ} \frac{p_0^2}{P^6 Q^2} - 2(d-1)Ne^4 \not\int_{PQ} \frac{1}{P^4 Q^2} \\ &\quad - \frac{2N(N+1)\lambda e^2}{3} \not\int_{PQ} \frac{1}{P^4 Q^2} + \frac{8N(N+1)\lambda e^2}{3} \not\int_{PQ} \frac{p_0^2}{P^6 Q^2}. \end{aligned} \quad (52)$$

The above sum-integrals are individually ultraviolet divergent. However, the poles in  $\epsilon$  cancel, and we are left with a finite result for  $\Pi_{00}^{(2)}(0)$ :

$$\Pi_{00}^{(2)}(0) = \frac{Ne^4T^2}{(4\pi)^2} + \frac{N(N+1)\lambda e^2T^2}{144\pi^2}. \quad (53)$$

The reason behind the fact that we get a finite result before renormalization is that the two counterterm diagrams cancel against each other as a consequence of the Ward identity. Using these results, we finally obtain  $m_E^2(\Lambda)$  to order  $e^4$  and  $\lambda e^2$ :

$$m_E^2(\Lambda) = \frac{Ne^2T^2}{3} \left[ 1 - \frac{2Ne^2}{3(4\pi)^2} \left( \ln \frac{\Lambda}{4\pi T} + \gamma_E + 1 \right) + \frac{3e^2}{(4\pi)^2} \right] + \frac{N(N+1)\lambda e^2T^2}{144\pi^2}. \quad (54)$$

In contrast with the scalar mass parameter,  $m_E^2(\Lambda)$  has no explicit dependence on  $\Lambda$ . This is easily verified by using the renormalization group equation for the gauge coupling  $e$ .

## 4 Middle-distance Coefficients

In this section we determine the middle-distance coefficients of MSQED, which is given by (4). We know from general renormalization theory that MSQED can reproduce the correlators of ESQED at long distances  $R \gg 1/eT$  to any desired accuracy by adding sufficiently many operators and tuning their coefficients as functions of the parameters of ESQED. The middle-distance coefficients are sensitive to momentum scales  $T$  and  $eT$ . The scale  $T$  has already been encoded in the parameters by the matching which was carried out in the previous section. In order to treat the physics on the scale  $eT$  correctly, we must include the mass parameter  $m_E^2(\Lambda)$  in the free part of the Lagrangian. By doing this, we treat the effects of  $m_E^2(\Lambda)$  to all orders, while the other parameters in ESQED are treated as perturbations. In particular this means that the scalar mass parameter is treated as a perturbation. Of course, this way of doing perturbative calculations is also afflicted with infrared divergences. However, these divergences are screened at the scale  $e^2T$ , to which the parameters of MSQED are insensitive. As long as we make the same incorrect assumptions about the long-distance behaviour in MSQED, we can use this method to determine the middle-distance coefficients of MSQED.

According to the discussion above, the Lagrangian of ESQED is split into a free and an interacting piece:

$$(\mathcal{L}_{\text{ESQED}})_0 = \frac{1}{4}F_{ij}F_{ij} + (\partial_i\phi^\dagger)(\partial_i\phi) + \frac{1}{2}(\partial_i\rho)^2 + \frac{1}{2}m_E^2(\Lambda)\rho^2 + \mathcal{L}_{\text{gf}} + \mathcal{L}_{\text{gh}}, \quad (55)$$

$$\begin{aligned} (\mathcal{L}_{\text{ESQED}})_{\text{int}} &= M^2(\Lambda)\phi^\dagger\phi + \frac{\lambda_E(\Lambda)}{6}(\phi^\dagger\phi)^2 + e_E^2(\Lambda)\phi^\dagger\phi A_i^2 + h_E^2(\Lambda)\phi^\dagger\phi\rho^2 \\ &+ ie_E(\Lambda)A_i(\phi^\dagger\partial_i\phi - \phi\partial_i\phi^\dagger) + \frac{\lambda_A(\Lambda)}{24}\rho^4 + \delta\mathcal{L}. \end{aligned} \quad (56)$$

Using strict perturbation theory the Lagrangian of MSQED is split in a way that is now familiar:

$$\begin{aligned}
(\mathcal{L}_{\text{MSQED}})_0 &= \frac{1}{4} \tilde{F}_{ij} \tilde{F}_{ij} + (\partial_i \tilde{\phi})^\dagger (\partial_i \tilde{\phi}) + \mathcal{L}_{\text{gf}} + \mathcal{L}_{\text{gh}}, \\
(\mathcal{L}_{\text{MSQED}})_{\text{int}} &= \tilde{M}^2(\Lambda) \tilde{\phi}^\dagger \tilde{\phi} + e_M^2(\Lambda) \tilde{\phi}^\dagger \tilde{\phi} \tilde{A}_i^{3d} \tilde{A}_i^{3d} + ie_M(\Lambda) \tilde{A}_i (\tilde{\phi}^\dagger \partial_i \tilde{\phi} - \tilde{\phi} \partial_i \tilde{\phi}^\dagger) + \\
&\quad \frac{\lambda_M(\Lambda)}{6} (\tilde{\phi}^\dagger \tilde{\phi})^2 + \delta \mathcal{L}'. \tag{57}
\end{aligned}$$

In MSQED, wiggly and solid lines denote the propagators of photons and charged scalars, respectively. Again, we only show the diagrams which are nonzero in the Landau gauge.

## 4.1 Field Normalization Constants

In the tree approximation the fields in ESQED and MSQED are related as

$$\tilde{\phi}(\Lambda) = \phi(\Lambda), \quad \tilde{A}_i(\Lambda) = A_i(\Lambda). \tag{58}$$

Again the field normalization constant can be read off from the momentum dependent part of the propagator of the underlying theory, which in this case is ESQED. Consider first the scalar field. In strict perturbation theory it is consistent to make a series expansion of the propagator in powers of the external momentum  $\mathbf{k}$ . The only mass scale provided in the loop integrals of ESQED is then the mass  $m_E^2(\Lambda)$ . Since the only one-loop diagram involving the field  $\rho$  is independent of the external momentum (the tadpole in Fig. 19), the one-loop correction to the momentum dependent part of the propagator vanishes. Hence there is no renormalization of the field  $\tilde{\phi}$ .

A similar argument holds for the gauge field: Since the interaction between the fields  $A_i$  and  $\rho$  gives rise to momentum dependent graphs first at the two-loop level, there is no renormalization of  $\tilde{A}_i$  at leading order in the coupling constants. Thus, (58) holds to next-to-leading order.

## 4.2 Coupling Constants

In this subsection we determine the gauge coupling  $e_M^2(\Lambda)$  and the quartic coupling  $\lambda_M(\Lambda)$  to next-to-leading order in the parameters of ESQED. The results for  $N = 1$  appear in Ref. [22]. The matching is somewhat simplified, since the fields in MSQED can be directly identified with the fields in ESQED to next-to-leading order.

Consider first the gauge coupling  $e_M^2(\Lambda)$ . This coefficient is determined by calculating the correlator  $\Gamma_{\Phi_1 \Phi_1 A_i A_j}^{\text{ESQED}}(0)$  and matching with the corresponding correlator in MSQED,

$\Gamma_{\Phi_1\Phi_1 A_i A_j}^{\text{MSQED}}(0)$ . The one-loop corrections to this correlator in ESQED only involve massless fields. Since the correlators are calculated at vanishing external momenta, the regularized loop integrals vanish. In MSQED, the same arguments apply equally well. We then conclude that the tree-level result holds at the one-loop level:

$$e_M^2(\Lambda) = e_E^2(\Lambda), \quad (59)$$

where  $e_E^2(\Lambda)$  is given by (36).

Let us next consider the coupling constant  $\lambda_M(\Lambda)$ . The quartic coupling  $\lambda_M(\Lambda)$  is determined by the following matching equation, in complete analogy with the calculations of  $\lambda_E(\Lambda)$  in subsection 3.2,

$$\Gamma_{\phi_1\phi_1\phi_1\phi_1}^{\text{ESQED}}(0) = \Gamma_{\phi_1\phi_1\phi_1\phi_1}^{\text{MSQED}}(0). \quad (60)$$

The only one-loop diagram contributing to  $\Gamma_{\phi_1\phi_1\phi_1\phi_1}^{\text{ESQED}}(\mathbf{k})$  at zero external momenta is displayed in Fig 18. The correlator in the one-loop approximation is

$$\Gamma_{\phi_1\phi_1\phi_1\phi_1}^{\text{ESQED}}(0) = \lambda_E(\Lambda) - 6e_E^4 \int_p \frac{1}{(p^2 + m_E^2)^2} \quad (61)$$

In MSQED, the one-loop corrections to the correlator  $\Gamma_{\phi_1\phi_1\phi_1\phi_1}^{\text{MSQED}}(\mathbf{k})$  vanish. Using the matching equation (60) and appendix B, we finally end up with

$$\lambda_M(\Lambda) = \lambda_E(\Lambda) - \frac{3e_E^4}{4\pi m_E}. \quad (62)$$

Here,  $\lambda_E(\Lambda)$  is given by (32).

### 4.3 Mass Parameter

In this subsection we determine the scalar mass parameter in the two-loop approximation. For  $N = 1$  this has previously been carried out in [22]. We calculate  $\tilde{M}^2(\Lambda)$  by matching the Higgs propagator in ESQED,  $\Gamma_{\phi_1, \phi_1}^{\text{ESQED}}(\mathbf{k})$  with the Higgs propagator in MSQED,  $\Gamma_{\phi_1, \phi_1}^{\text{MSQED}}(\mathbf{k})$ . The diagrams contributing to the two-point function in the strict perturbation expansion of ESQED are displayed in Fig. 19. After Taylor expanding the self-energy function in ESQED in powers of  $k^2$ , the mass  $m_E^2(\Lambda)$  is the only mass scale in the loop diagrams. This implies that all loop diagrams which does not involve the field  $\rho$  vanish in dimensional regularization. The two-point function in ESQED then reads

$$\begin{aligned} \Gamma_{\phi_1, \phi_1}^{\text{ESQED}}(\mathbf{k}) &= k^2 + M^2(\Lambda) + e_E^2 \int_p \frac{1}{p^2 + m_E^2} - \\ &2e_E^4 \int_{pq} \frac{1}{(p^2 + m_E^2)(q^2 + m_E^2)(\mathbf{p} + \mathbf{k} - \mathbf{q})^2}. \end{aligned} \quad (63)$$

The one-loop diagrams in MSQED are the same as in ESQED, except for those diagrams which involve the real scalar field  $\rho$ . Thus, the loop corrections to scalar self-energy function in strict perturbation theory, vanish and the only non-vanishing contribution comes from the mass counterterm  $\delta\tilde{M}^2$ , which cancels the logarithmic ultraviolet divergence

$$\Gamma_{\phi_1, \phi_1}^{\text{MSQED}}(\mathbf{k}) = k^2 + \tilde{M}^2(\Lambda) + \delta\tilde{M}^2. \quad (64)$$

Matching the two expressions, (63) and (64) we find

$$\tilde{M}^2(\Lambda) = M^2(\Lambda) + e_E^2 \int_p \frac{1}{p^2 + m_E^2} - 2e_E^4 \int_{pq} \frac{1}{(p^2 + m_E^2)(q^2 + m_E^2)(\mathbf{p} - \mathbf{q})^2} - \delta\tilde{M}^2. \quad (65)$$

The integrals are tabulated in Appendix B. The two-loop integral is ultraviolet divergent. The pole in  $\epsilon$  must then be canceled by the mass counterterm, which then is determined to be

$$\delta\tilde{M}^2 = \frac{e_E^4}{2(4\pi)^2\epsilon}. \quad (66)$$

Our final expression for the scalar mass parameter in MSQED is

$$\tilde{M}^2(\Lambda) = M^2(\Lambda) - \frac{e_E^2 T m_E}{4\pi} - \frac{e_E^4}{16\pi^2} \left[ 1 + 2 \ln \frac{\Lambda}{2m_E} \right]. \quad (67)$$

Here,  $M^2(\Lambda)$  is given by (48)

## 5 Summary

In the present paper we have discussed the dimensional reduction approach to hot field theories which has been developed into a quantitative tool by Farakos *et al.* [22] and by Braaten and Nieto [23]. The basic idea is to exploit the fact there are two or more well-separated mass scales in the system and that the heavy degrees of freedom decouple at long distance leaving us with effective field theories of the light degrees of freedom. The effects of the heavy modes are to renormalize the parameters in the effective theory and to induce new higher order interactions.

In this work I have applied this method to a field theory consisting of  $N$  charged  $U(N)$  symmetric scalars coupled to an abelian gauge field. I have presented the calculations of the parameters of ESQED and MSQED to next-to-leading order in the parameters  $\nu^2$ ,  $\lambda$  and  $e^2$  of full SQED. The results are a generalization of existing results for  $N = 1$  [22].

The effective field theory (MSQED) that we have obtained can now be used for a non-perturbative study of the phase transition on the lattice. This includes in particular the order of the phase transition as a function of the number of scalar fields  $N$ . The results could be compared to the findings of the  $\epsilon$ -expansion, and give some useful information on the applicability of this method.

# Acknowledgements

The author would like to thank Eric Braaten for useful discussions and suggestions.

## A Sum-integrals in the Full Theory

Throughout the work we use the imaginary time formalism, where the four-momentum is  $P = (p_0, \mathbf{p})$  with  $P^2 = p_0^2 + \mathbf{p}^2$ . The Euclidean energy takes on discrete values,  $p_0 = 2n\pi T$  for bosons and  $p_0 = (2n + 1)\pi T$  for fermions. Dimensional regularization is used to regularize both infrared and ultraviolet divergences by working in  $d = 4 - 2\epsilon$  dimensions, and we apply the  $\overline{MS}$  renormalization scheme. We shall use the following notations for the sum-integrals that appear

$$\rlap{-}\int_P f(P) \equiv \left(\frac{e^{\gamma_E} \mu^2}{4\pi}\right)^\epsilon T \sum_{p_0=2\pi n T} \int \frac{d^{3-2\epsilon} p}{(2\pi)^{3-2\epsilon}} f(P). \quad (\text{A.1})$$

The one-loop sum-integrals needed in this work have been calculated in e.g. Ref. [10]. We list them here for the convenience of the reader:

$$\rlap{-}\int_P \frac{1}{P^2} = \frac{T^2}{12} \left(\frac{\mu}{4\pi T}\right)^{2\epsilon} \left[1 + \left(2 + 2\frac{\zeta'(-1)}{\zeta(-1)}\right)\epsilon + \mathcal{O}(\epsilon^2)\right], \quad (\text{A.2})$$

$$\rlap{-}\int_P \frac{1}{(P^2)^2} = \frac{1}{(4\pi)^2} \left(\frac{\mu}{4\pi T}\right)^{2\epsilon} \left[\frac{1}{\epsilon} + 2\gamma_E + \mathcal{O}(\epsilon)\right], \quad (\text{A.3})$$

$$\rlap{-}\int_P \frac{P_0^2}{(P^2)^2} = -\frac{T^2}{24} \left(\frac{\mu}{4\pi T}\right)^{2\epsilon} \left[1 + 2\frac{\zeta'(-1)}{\zeta(-1)}\epsilon + \mathcal{O}(\epsilon^2)\right], \quad (\text{A.4})$$

$$\rlap{-}\int_P \frac{P_0^2}{(P^2)^3} = \frac{1}{4(4\pi)^2} \left(\frac{\mu}{4\pi T}\right)^{2\epsilon} \left[\frac{1}{\epsilon} + 2 + 2\gamma_E + \mathcal{O}(\epsilon)\right], \quad (\text{A.5})$$

$$\rlap{-}\int_P \frac{P_0^4}{(P^2)^4} = \frac{1}{8(4\pi)^2} \left(\frac{\mu}{4\pi T}\right)^{2\epsilon} \left[\frac{1}{\epsilon} + \frac{8}{3} + 2\gamma_E + \mathcal{O}(\epsilon)\right]. \quad (\text{A.6})$$

Here,  $\gamma_E$  is the Euler-Mascheroni constant and  $\zeta(x)$  is the Riemann Zeta function.

Arnold and Zhai [10], and Kastening and Zhai [11] have calculated and tabulated all the two-loop sum-integrals, except for the last one, in the list below.

$$\rlap{-}\int_{PP} \frac{1}{P^2 Q^2 (P+Q)^2} = 0, \quad (\text{A.7})$$

$$\rlap{-}\int_{PP} \frac{q_0^2}{P^4 Q^2 (P+Q)^2} = \frac{T^2}{12(4\pi)^2} + \mathcal{O}(\epsilon), \quad (\text{A.8})$$

$$\not\int_{PP} \frac{p_0^2}{P^4 Q^2 (P+Q)^2} = 0, \quad (\text{A.9})$$

$$\not\int_{PP} \frac{p_0 q_0}{P^2 Q^4 (P+Q)^2} = 0. \quad (\text{A.10})$$

The last integral can, however, be found from the second and third by changing variables.

## B Integrals in the three Dimensional Theory

In the effective three-dimensional theory we use dimensional regularization in  $3 - 2\epsilon$  dimensions to regularize infrared and ultraviolet divergences. In analogy with Appendix A, we define

$$\int_p f(p) \equiv \left(\frac{e^{\gamma_E} \mu^2}{4\pi}\right)^\epsilon \int \frac{d^{3-2\epsilon} p}{(2\pi)^{3-2\epsilon}} f(p). \quad (\text{B.1})$$

Again  $\mu$  coincides with the renormalization scale in the modified minimal subtraction renormalization scheme.

In the effective theory we need the following one-loop integrals

$$\int_p \frac{1}{p^2 + m^2} = \frac{m}{4\pi} \left(\frac{\mu}{2m}\right)^{2\epsilon} [-1 - 2\epsilon + \mathcal{O}(\epsilon^2)], \quad (\text{B.2})$$

$$\int_p \frac{1}{(p^2 + m^2)^2} = \frac{1}{4\pi m} \left(\frac{\mu}{2m}\right)^{2\epsilon} \left[\frac{1}{2} + \mathcal{O}(\epsilon^2)\right]. \quad (\text{B.3})$$

All integrals are straightforward to evaluate in dimensional regularization. Details may be found in Ref. [37]. The specific two-loop integrals needed are

$$\int_{pq} \frac{1}{(p^2 + m^2)(q^2 + m^2)(\mathbf{p} - \mathbf{q})^2} = \frac{1}{16\pi^2} \left[\frac{1}{4\epsilon} + \frac{1}{2} + \frac{\mu}{2m} + \mathcal{O}(\epsilon)\right].$$

This integral have been computed by several authors, e.g. in Ref. [5].

## References

- [1] L. Dolan and R. Jackiw, Phys. Rev. **D 9**, 3320, 1974.
- [2] E. Braaten and R. Pisarski, Nucl. Phys. **B 337**, 569, 1990.
- [3] A. Hebecker, Z. Phys. **C 60**, 271, 1993.

- [4] Z. Fodor and A. Hebecker, Nucl. Phys. **B432**, 127, 1994.
- [5] P. Arnold and O. Espinosa, Phys. Rev. **D 47**, 3546, 1993.
- [6] J. Frenkel, A. V. Saa and J. C. Taylor, Phys. Rev. **D 46**, 3670, 1992.
- [7] R. Parwani, Phys. Rev. **D 51**, 4518, 1995.
- [8] C. Corianò and R. Parwani, Nucl. Phys. **B 434**, 56-84, 1995.
- [9] R. Parwani, Phys. Lett. **B 334**, 420, 1994, ERRATUM-ibid. **B 342**, 454, 1995.
- [10] P. Arnold and C. Zhai, Phys. Rev. **D 50**, 7603, 1994; Phys. Rev. **D 51**, 1906, 1995.
- [11] C. Zhai, B. Kastening, Phys. Rev. **D 52**, 7232, 1995.
- [12] P. Arnold and L. G. Yaffe, Phys. Rev. **D 49**, 3003, 1994.
- [13] I. Lawrie, Nucl. Phys. **B 200**, 1, 1982.
- [14] T. Appelquist and Carrazone, Phys. Rev. **D 11**, 2856, 1975.
- [15] J. March-Russell, Phys. Lett. **B 296**, 364, 1992.
- [16] M. Alford and J. March-Russell, Nucl.Phys. **B 417**, 527, 1994.
- [17] G. P. Lepage, in *From actions to answers*, proceedings of the Advanced Study Institute in Elementary Particle Physics, Boulder, Colorado, 1989, edited by T. De-Grand and D. Toussaint, World Scientific, 1989.
- [18] D. J. Gross, R. D. Pisarski and L. G. Yaffe, Rev. Mod. Phys. **53**, 43, 1981.
- [19] N. P. Landsman. Nucl. Phys. **B 322**, 498, 1989.
- [20] T. Appelquist and R. Pisarski, Phys. Rev. **D 23**, 2305, 1981
- [21] S. Nadkarni, Phys. Rev. **D 27**, 917.
- [22] K. Farakos, K. Kajantie, K. Rummukainen, M.Shaposhnikov. Nucl. Phys. **B 425**, 67, 1994.
- [23] E. Braaten and A. Nieto, Phys. Rev. **D 51**, 6990, 1995.
- [24] K. Farakos, K. Kajantie, K. Rummukainen and M. Shaposhnikov, Nucl. Phys. **B 442**, 317, 1995.
- [25] K. Kajantie, M. Laine, K. Rummukainen, M. Shaposhnikov, Nucl. Phys. **B 458**, 90, 1996.

- [26] K. Kajantie, M. Laine, K. Rummukainen and M. Shaposhnikov, Phys. Rev. Lett. **77**, 2877, 1996.
- [27] V. A. Kuzmin, V. A. Rubakov and M. E. Shaposhnikov, Phys. Lett. **B 155**, 36, 1985.
- [28] M. E. Shaposhnikov, Nucl. Phys. **B 287**, 757, 1987.
- [29] D. Bödeker, P. John, M. Laine, and M. G. Schmidt, Nucl. Phys. **B 497**, 387, 1997.
- [30] E. Braaten and A. Nieto, Phys. Rev. **D 53**, 3421, 1996.
- [31] A. D. Linde, Rep. Prog. Phys. **42**, 389, 1979.
- [32] J. O. Andersen, Phys Rev. **D 53**. 7286, 1996.
- [33] J. O. Andersen, Z. Phys. **C 75**, 147, 1997; Ph. D. thesis, University of Oslo, 1997.
- [34] M. Karjalainen, M. Laine and J. Peisa, Nucl. Phys. Proc. Suppl. **53**, 475, 1997.
- [35] K. Kajantie, M. Karjalainen, M. Laine and J. Peisa, cond-mat/9704056; hep-lat/9711048.
- [36] A. Jakovác, Phys. Rev. **D 53**, 4538, 1996.
- [37] L. H. Ryder, *Quantum Field Theory*, Cambridge University Press, Cambridge, 1985.
- [38] J. I. Kapusta, *Finite Temperature Field Theory*, Cambridge University Press, Cambridge, 1989.

FIGURE CAPTIONS:

Figure 1: The tadpole in scalar theory.

Figure 2: One-loop scalar self-energy diagrams in the full theory.

Figure 3: One-loop diagrams for the photon polarization tensor in the full theory.

Figure 4: Two-loop scalar self-energy diagrams in SQED.

Figure 5: Two-loop self-energy diagrams for the timelike component of the gauge field in SQED.

Figure 6: One-loop graphs contributing to the scalar four-point function in the full theory.

Figure 7: One-loop diagrams needed for the calculating the couplings  $e_E^2(\Lambda)$  and  $h_E^2(\Lambda)$ .

Figure 8: One-loop diagrams contributing to the four-point function of  $\rho$  in SQED.

Figure 9: One and two-loops diagram contributing to the scalar self-energy function in ESQED.

Figure 10: One-loop diagram relevant for the calculation of scalar self-coupling in ESQED.

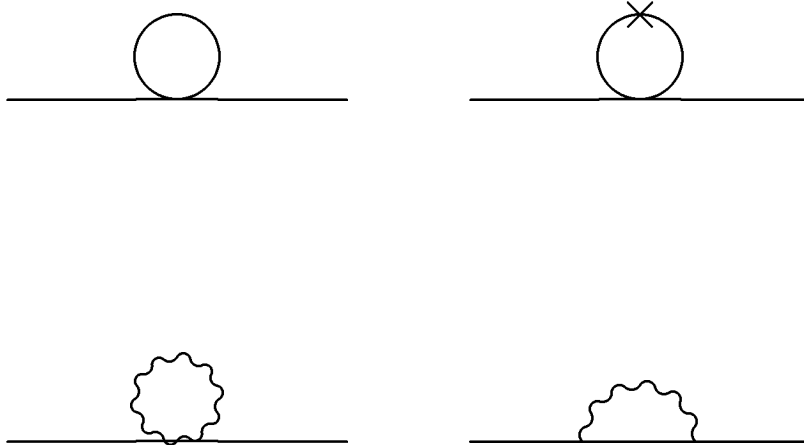


Figure 11: One-loop scalar self-energy diagrams in the full theory.

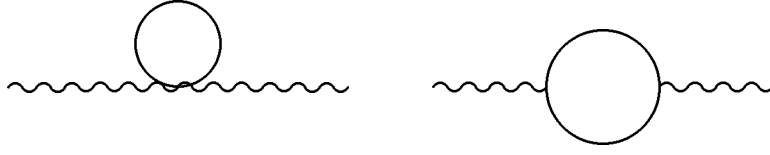


Figure 12: One-loop diagrams for the photon polarization tensor in the full theory.



Figure 13: One-loop graphs contributing to the scalar four-point function in the full theory.

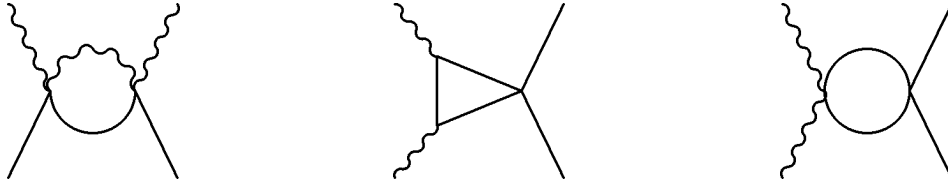


Figure 14: One-loop diagrams needed for the calculating the couplings  $e_E^2(\Lambda)$  and  $h_E^2(\Lambda)$ .

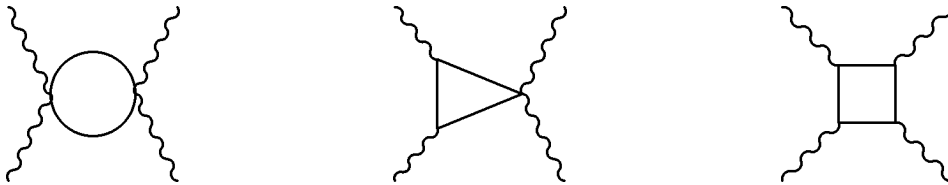


Figure 15: One-loop diagrams contributing to the four-point function of  $\rho$  in SQED.

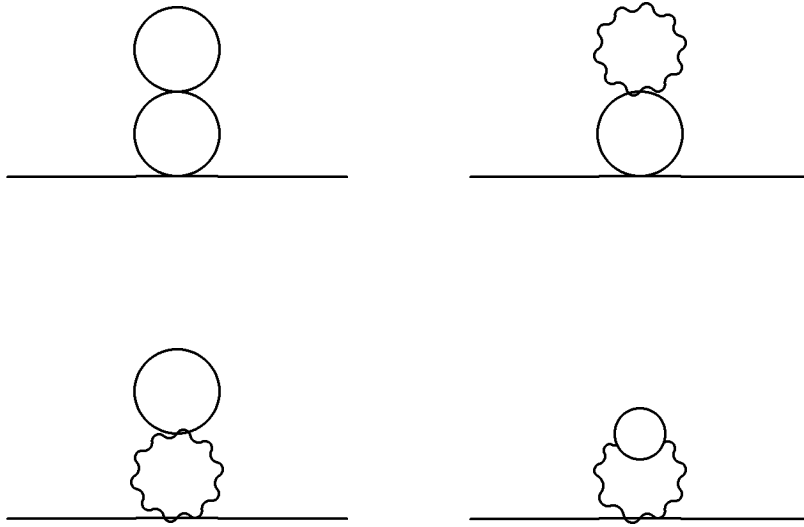


Figure 16: Two-loop scalar self-energy diagrams in SQED.

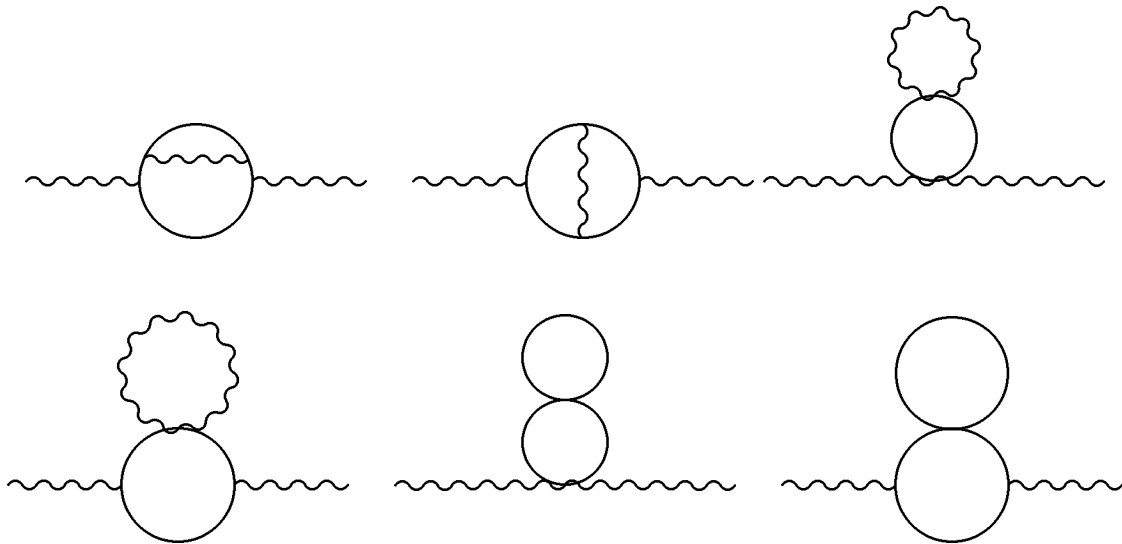


Figure 17: Two-loop self-energy diagrams for the timelike component of the gauge field in SQED.

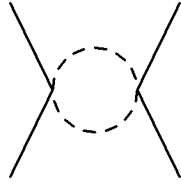


Figure 18: One-loop diagram relevant for the calculation of scalar self-coupling in ESQED.

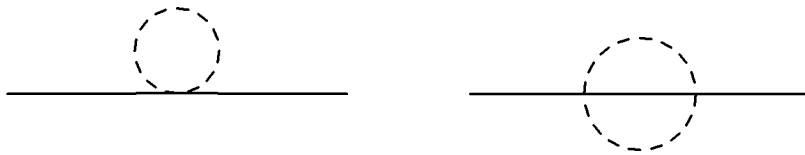


Figure 19: One and two-loops diagram contributing to the scalar self-energy function in ESQED.